REPORT DOCUMENTATION PAGE

Form Approved
OMB No. 0704-0188

1. AGENCY USE ONLY (Leave blank)	2. REPORT DATE	3. REPORT TYPE AND DATES COVERED
	4/29/99	Final Technical Report, 2/98-3/99

4. TITLE AND SUBTITLE

Chemical Flame Suppression by Phosphorus-Containing Compounds

5. FUNDING NUMBERS

DASW01-98-C-0015

4D/3/9

6. AUTHOR(S)

E.M. Fisher, J.W. Gillett, F.C. Gouldin, T.M. Jayaweera, M.A. MacDonald

7. PERFORMING ORGANIZATION NAME(S) AND ADDRESS(ES)

Cornell University, Sibley School of Mechanical and
Aerospace Engineering, Upson Hall, Ithaca, NY 14853-7501

8. PERFORMING ORGANIZATION REPORT NUMBER

9. SPONSORING/MONITORING AGENCY NAME(S) AND ADDRESS(ES)

Defense Advance Research Projects Agency (DARPA)
3701 North Fairfax Drive,
Arlington, VA 22203-1714

10. SPONSORING/MONITORING AGENCY REPORT NUMBER

11. SUPPLEMENTARY NOTES

12a. DISTRIBUTION/AVAILABILITY STATEMENT

Unlimited

DISTRIBUTION STATEMENT A
Approved for Public Release
Distribution Unlimited

13. ABSTRACT *(Maximum 200 words)*

Several techniques were used to aid in the assessment of PCCs as flame suppressants: GC/MS with chemical derivatization, a qualitative toxicology assessment of the byproducts, measurements of the global extinction strain rate, emission spectroscopy. We also developed two important new capabilities: (1) laser-induced fluorescence (LIF) to measure concentrations of OH (a key flame radical) as a measure of suppressant effectiveness and as a means of understanding the mechanism of flame suppression, and (2) droplet generation and feed systems to enable the future evaluation of low-vapor-pressure PCCs as liquids or aqueous solutions. Diethyl methylphosphonate and dimethyl phosphonate were tested as vapor-phase additives. Their effect on the global extinction strain rates of the methane/air flames indicated that they had flame-suppression effectivenesses very similar to those of the PCCs tested previously. The following stable byproducts were identified in a methane/air flame doped with DMMP: methyl methylphosphonate, $P(=O)(-CH_3)(-OCH_3)(-OH)$; dimethyl phosphate, $P(=O)(-OCH_3)_2(-OH)$; monomethyl phosphate, $P(=O)(-OCH_3)(-OH)_2$; methylphosphonic acid, $P(=O)(-CH_3)(-OH)_2$; phosphonic acid, $P(=O)(-H)(-OH)_2$; phosphorous acid, $P(-OH)_3$; orthophosphoric acid, $P(=O)(-OH)_3$, none of which is highly neurotoxic. A continuum emission and features associated with PO and PH were identified in emission spectra in DMMP-doped methane/air flames. Preliminary OH LIF and electrospray results are presented.

14. SUBJECT TERMS	15. NUMBER OF PAGES
flame suppression, phosphorus, extinction, halon replacement, opposed-jet diffusion flame	30
	16. PRICE CODE

17. SECURITY CLASSIFICATION OF THIS REPORT	18. SECURITY CLASSIFICATION OF THIS PAGE	19. SECURITY CLASSIFICATION OF ABSTRACT	20. LIMITATION OF ABSTRACT
Unclassified	Unclassified	Unclassified	UL

I. SUMMARY

I A. Task Objectives

This project had two general objectives: (1) to generate information leading to a more informed assessment of phosphorus-containing compounds (PCCs) as flame suppressants, and (2) to develop new capabilities that can contribute in the future to the testing of low-volatility flame suppressants and the understanding of the mechanism of PCC flame suppression. The specific approaches to these objectives are described in Section I C. below.

I B. Technical Problems

PCCs are highly effective flame suppressants that have been studied comparitively little. Difficulties in assessing their potential as halon replacements stem from the poor state of development of techniques for delivering them to flames, and for measuring them and their stable and short-lived products and byproducts.

I C. General Methodology

We used many different techniques to generate new information to aid in the assessment of PCCs as flame suppressants: We used GC/MS with chemical derivatization to identify stable combustion products and byproducts of dimethyl methylphosphonate (DMMP) in an opposed-jet methane-air non-premixed flame. We performed a qualitative toxicology assessment of the byproducts that we identified. We measured the global extinction strain rate of a methane/air flame doped with vapor-phase PCCs that we had not studied previously (Fisher et al., 1998). We used emission spectroscopy to identify some transient phosphorus-containing species present in the flame; For one of these transient species, we determined how the strength of the emission feature varied with phosphorus loading and strain rate.

We also developed two important new capabilities: (1) laser-induced fluorescence (LIF) to measure concentrations of OH (a key flame radical) as a measure of suppressant effectiveness and as a means of understanding the mechanism of flame suppression, and (2) droplet generation and feed systems to enable the future evaluation of low-vapor-pressure PCCs as liquids or aqueous solutions.

I D. Technical Results

Two new PCCs, diethyl methylphosphonate and dimethyl phosphonate, were tested as flame suppressants, as vapor-phase additives. Their effect on the global extinction strain rates of the methane/air flames into which they were introduced indicated that they had flame-suppression effectivenesses very similar to those of the PCCs we had tested previously (Fisher et al., 1998). See Section III B for more information.

The following stable byproducts were identified in a methane/air flame doped with DMMP: methyl methylphosphonate, $P(=O)(-CH_3)(-OCH_3)(-OH)$; dimethyl phosphate, $P(=O)(-OCH_3)_2(-OH)$; monomethyl phosphate, $P(=O)(-OCH_3)(-OH)_2$; methylphosphonic acid, $P(=O)(-CH_3)(-OH)_2$; phosphonic acid, $P(=O)(-H)(-OH)_2$; phosphorous acid, $P(-OH)_3$; orthophosphoric acid, $P(=O)(-OH)_3$. See Section III C for more information about the identification of these compounds. Section III D contains a qualitative assessment of their toxicity, focusing on neurotoxicity.

Features associated with PO and PH were identified in emission spectra in DMMP-dope methane/air flames. A continuum emission was also observed. The strength of the PO emission feature increased with increased DMMP loading, but will probably not be very useful for quantifying the phosphorus levels present in the flame. See Section III E for details.

Several tests have been performed to assess the performance of the new OH LIF and electrospray systems. These tests are described in Sections III F, G, and H below.

I E. Important Findings and Conclusions

Our findings support the hypothesis that PCCs' flame suppression is insensitive to their initial chemical form, and is probably due to effects on radical chemistry in the flame zone. However, the experiments reported here do not provide a definitive test of that hypothesis.

No highly neurotoxic toxic combustion byproducts of DMMP were identified. Such a finding would have disqualified DMMP, and probably most similar compounds, from consideration as halon replacements. Corrosive acid combustion products were

identified, and are likely to pose a threat comparable to that resulting from halon flame suppression.

Preliminary results of OH LIF and electrospray droplet delivery indicate that these techniques can contribute to future studies of PCC flame suppression.

I F. Significant Hardware Developments

We developed two new hardware systems that can be used in the future to investigate flame suppression effectiveness and mechanisms for PCCs and other candidate halon replacements. Laser-induced fluorescence capabilities for measuring OH radicals are described in Section III A 5 below, with preliminary results given in Section III F below. This instrumentation provides spatially resolved, quantitative, data on OH levels in the flame, allowing comparisons of flame radical levels in the presence of PCC dopants to levels in undoped flames. Electrospray droplet delivery capabilities are described in Section III A 4 below, with preliminary results given in Section III G and III H below. The electrospray apparatus has the potential to deliver low-volatility flame suppressants to a laboratory flame in a nearly monodisperse spray of small droplets -- the ideal form for investigating their chemical effectiveness. Further work is needed before this potential can be realized for the PCCs we have investigated.

I G. Special Comments

none

I H. Implications for Future Research

Further research on PCCs is merited. Of particular importance are tests of the flame suppression effectiveness of compounds with a wider range of molecular structures than those studied to date. Investigations of the mechanism of flame suppression are also needed.

II. ARTICLES PUBLISHED

No new papers were submitted for publication during this project. However, two papers that had been submitted for publication in the previous, related, one-year project

(Fisher et al., 1998) appeared in print in the archival literature during the current project. Their bibliographical references follow:

1. MacDonald, M.A, Jayaweera, T.M., Fisher, E.M., and Gouldin, F.C., "Inhibition of Non-Premixed Flames by Phosphorus-Containing Compounds," *Combustion and Flame*, v.116, pp. 166-176 (1999).

2. MacDonald, M.A, Jayaweera, T.M., Fisher, E.M., and Gouldin, F.C., "Variation of Chemically Active and Inert Flame Suppression Effectiveness with Stoichiometric Mixture Fraction," *27th Symposium (International) on Combustion The Combustion Institute*, pp. 2749-2756 (1998).

III. DETAILED PROJECT DESCRIPTION

III A. Experimental Apparatus and Techniques

III A 1. Burners and Extinction Measurement

Two opposed-jet burners systems were used for the experiments reported here. The first, referred to here as Burner I, was used for extinction measurements, extractive sampling, spectral emission measurements, and electrospray experiments. This burner and feed system are described in detail in Section III A of Fisher et al. (1998). Modifications of Burner I for electrospray experiments are detailed below, in Section III A 4. The technique for approaching extinction and the expression for global strain rate are unchanged from Fisher et al. (1998). All extinction measurements were performed with reactants at 100 °C.

The second burner, Burner II, was used for laser-induced fluorescence (LIF) measurements and PO emission spectroscopy profiles. This burner facility, which was built for the current project, has a burner nozzle geometry almost identical to that of Burner II, but incorporates many improvements to the housing to facilitate accurate optical measurements. The only geometrical differences are larger tubes for sheath flow (1.5" vs 1.0 "), larger offset in the upstream direction of the sheath flow tube exit with respect to the main flow tube exit (0.5" vs. 0.25"), and a longer air flow tube length. Extinction strain rate measurements for undoped methane-air flames taken in the two

burner facilities agree to within 3%, confirming the similarity of the two systems. All of the key features of the original burner system are kept: active temperature control of the reactant streams in the nozzles, heating of reactant lines, syringe pump dopant injection, spark ignition system and nitrogen purge flow for the housing. The new burner uses an improved alignment mechanism for the reactant tubes. The mechanism has 3 degrees of freedom, allowing the upper nozzle to be moved roughly 5mm in any transverse direction and more than 30mm in the vertical direction. Once aligned the nozzles are held rigidly in place allowing for long term stability of the configuration. This system also allows for the gap size to be adjusted and measured to within 0.05mm. Optical improvements include a large (100mm viewable diameter) quartz window for fluorescence collection. This window is mounted at 90 degrees to the laser axis. Two smaller (25mm) quartz windows allow the laser beam to pass straight through the burner housing. (See Fig. 3., below.) The entire burner, including collection optics was mounted on a lathe bed allowing it to be laterally traversed for final alignment.

III A 2. Extractive Measurements of Stable Products

Extractive sampling, coupled with derivatization, was used with a GC/MS to identify stable combustion byproducts of non-premixed flames doped with DMMP [CAS 756-79-6]. To extract the compounds, a straight quartz probe with an orifice of 125μm, ID=3.8mm, and OD=6.3mm was inserted into the side of the chamber in which our burner is housed. The length of the probe was 30 cm, determined by the length of the chamber arm. The probe was inserted radially, in the same plane as the flame. It was held stationary in a region of high temperature, determined by the glowing of the probe tip. The radial position of the probe was chosen to place the orifice near the edge of the chemiluminescent flame zone. This prevented quenching the flame by the probe. Once the probe was positioned, the sampling began using the procedure as described by Rapp et al. (1997), with several modifications: Firstly, no internal standard was used with the BSTFA/TMCS derivatization agent. Secondly, the nitrogen-drying process was eliminated to avoid losing volatile compounds. Instead, the liquid from the trapping tube was poured into a small glass vial before the tube was washed with 2ml of BSTFA mixture. The contents of the trapping tube were added to the liquid in the vial, along

with extra (~1ml) BSTFA/TMCS such that the ratio of water to BSTFA/TMCS was at most 1:25. This procedure was adopted so that no solid phase would be formed. The resulting liquid was injected into the GC/MS and analyzed in the same manner as described by Rapp et al. (1997). A test was also done in which the walls of the burner housing were scraped with a stainless steel spatula, the collected material put in a small vial and mixed with the BSTFA/TMCS and similarly injected into the GC/MS. Also, the sampling probe was washed directly with the BSTFA/TMCS and analyzed. The GC and MSD are both HP series 6890.

III A 3.Emission Spectroscopy

Spectra of light emitted from flames doped with DMMP were acquired using a Jarrell Ash 1/4m monochromator and an EMI 9781B photomultiplier tube. The monochromator was operated with two different gratings, the low-blaze grating optimized for 300 nm light, and the high-blaze grating with its peak response at 600 nm. The spectral resolution was approximately 1 nm FWHM. The spectral response of the PMT covered the range 620-200nm. Emission spectra were taken using computer control of monochromator scanning and data acquisition. The image of the flame from Burner I was focused onto the entrance slit of the monochromator using a 200-mm focal length quartz lens.

The emitted light from a particular feature (the PO emission band at 325 nm) was examined in more detail, in spatially resolved measurements in Burner II. The basic configuration of Burner II was the same as for the laser-induced fluorescence measurements (See section III A 5.). Two major modifications were required for this study: (1) the replacement of the LIF photomultiplier tube, which is not suitable for steady state measurements, with the EMI 9781B tube and a 3.3 Mohm load resistor, and (2) the use of a 325nm bandpass (10nm FWHM) filter in place of the colored glass filters. Steady voltage output from the pmt was measured using an HP 3478A multimeter. In contrast to the visible emission work done with the original opposed jet burner, the new set up provides a 100 μm spatial resolution with a high repeatability.

III A 4. Electrospray Apparatus

The electrospray experiment was implemented by modifying the upper tube of Burner I. The modified burner tube is shown in Fig. 1, which is not to scale. The electrospray apparatus consists of three tubes that lie concentrically along the axis of the air flow tube of the burner. The inner, capillary, tube carries the liquid to be sprayed, which is delivered via a syringe pump. This tube is made of non-conductive fused silica to ensure that the syringe pump is electrically isolated from the high voltage required for the electrospray. The middle, metal, tube is maintained at high voltage, and is insulated from the other parts of the burner by the outer, PEEK polymer, tube. The tubes are held in place by a teflon spacer disk perforated with an array of 0.3-mm holes. The ground electrode consists of a 2-mm ring of conductive paint on the inside of the air flow tube. The high voltage source for electrospraying is a Bertan Model 205B-10R 10 kV power supply. The position of the spraying apparatus varied in the different tests: The distance between the exit of the flow tube and the grounding ring was: 5 cm for droplet size measurements with DMMP, 0 cm for droplet size measurements with aqueous solutions of PCCs, and 10 cm for extinction tests. The distance between the capillary tip and the grounding ring remained 3 mm for all experiments reported here, except for the droplet extinction measurements, for which it was 5 mm. Not shown in Fig. 1 is the annulus, outside the main flow tube, through which nitrogen can flow. This annulus and the accompanying sheath flow was present for all extinction measurements, but was absent in all the droplet size measurements and flow visualization experiments.

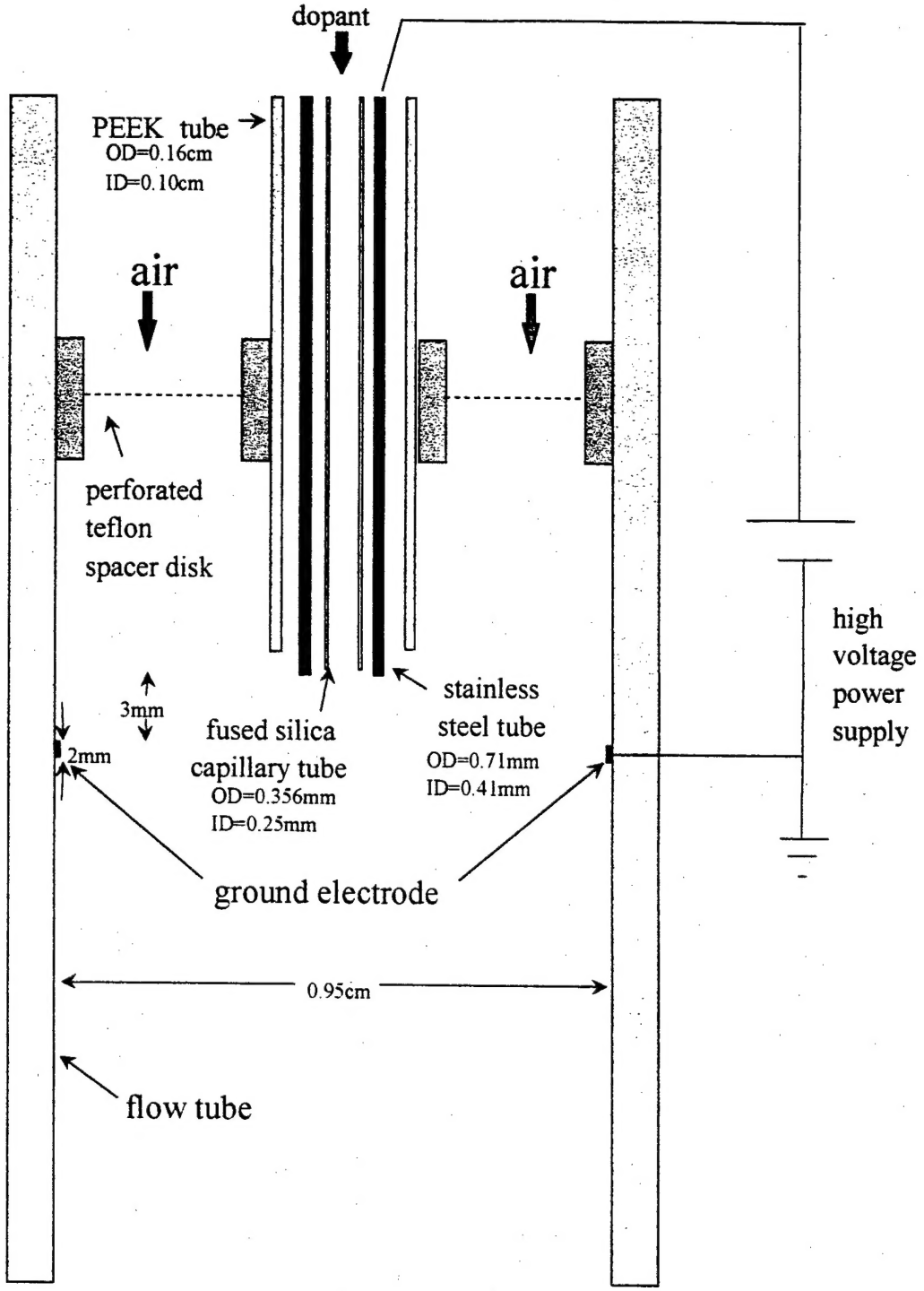

Fig. 1. Electrospray apparatus.

Laser sheet visualization of the sprayed liquid was used to select conditions of operation of the electrospray. These experiments took place in a simulated burner flow tube with a single quartz wall, because the burner did not provide adequate optical access. Figure 2 shows the layout of the laser sheet visualization experiments. A mirror was placed at 45 degrees below the spray, and a glass rod, acting as a cylindrical lens, was placed directly above the mirror. The laser was positioned horizontally so that it would strike the mirror, be reflected 90 degrees upward, and hit the glass rod, diverging into a sheet that illuminated the spray in the flow tube.

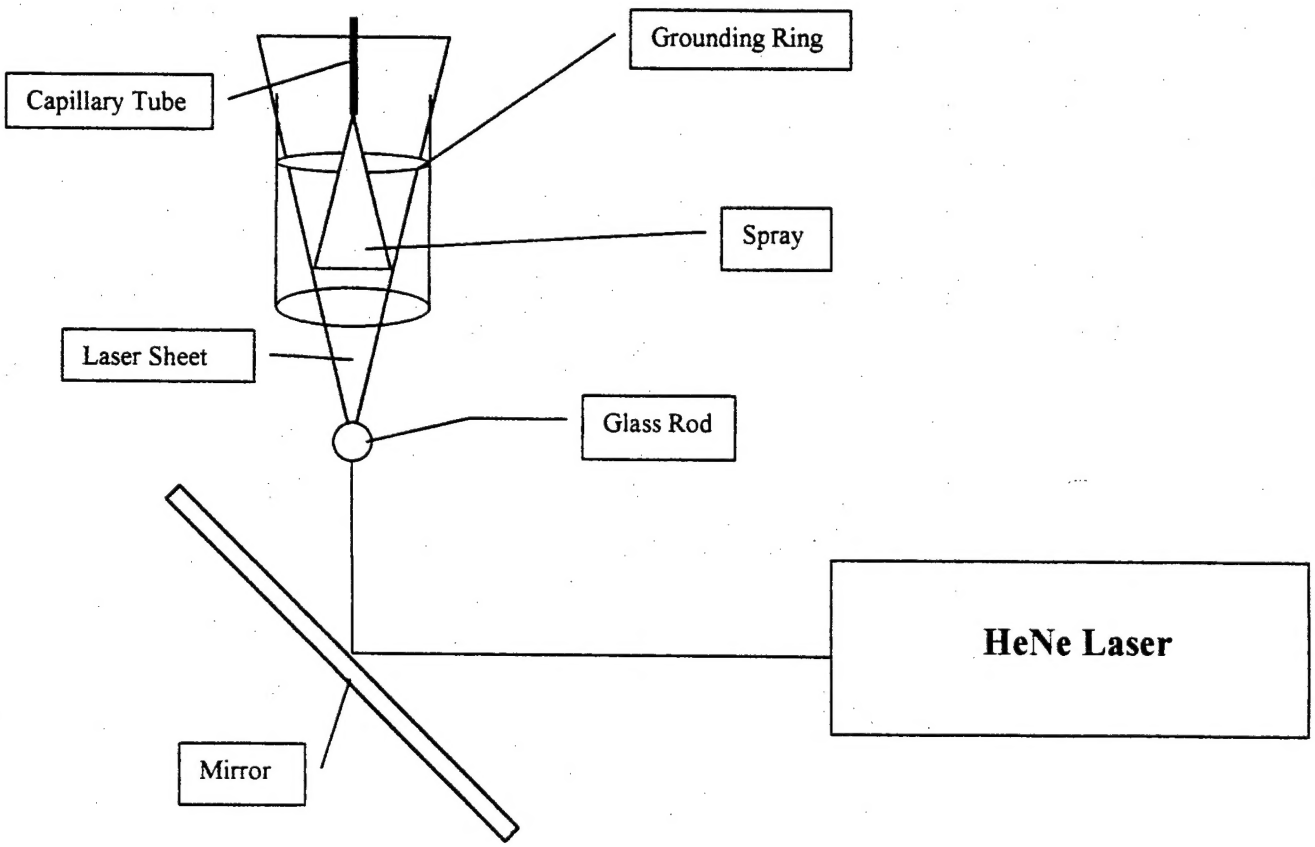

Fig. 2. Side view of spray visualization apparatus

III A 5.Laser-Induced Fluorescence

The LIF system is shown in Fig. 3. A frequency doubled Nd:YAG laser (Spectra Physics, DCR 2A) pumps a dye laser (Quanta Ray, PDL 2) which uses the R590 dye to produce light near 560nm. The output from the dye laser is then frequency doubled using a KD*P crystal, producing an ultraviolet beam near 280nm. This beam is then separated from the visible beam, focused into a sheet and directed into the combustion chamber, where it excites the A ← X (1,0) $Q_1(8)$ electronic transition in the OH molecule. The intensity of the laser radiation is chosen to be low enough to avoid saturation of the absorbing transition, thus yielding a fluorescence signal that is approximately proportional (uncorrected for changes in local quenching environment) to the ground state population of the excited rotational level. A fraction of the excited molecules fluoresce in the (0,0) and (1,1) bands of the A ← X transition, producing light in the 305-325 nm region. This light is detected by a photomultiplier tube located behind two colored glass filters (Schott UG-11 and WG-305), which discriminate against the laser radiation. The collection optics and a 100-μm slit are mounted on vertical traverse, allowing the detector to sample from different regions across the flame. This configuration is shown in Fig. 3. Our current measurements are uncorrected for spatial variations in photocathode response and laser intensity across the illuminated sheet. We intend to use LIF of acetone in a well-mixed configuration to calibrate our system to these spatial variations. In the future, we will convert the resulting relative OH profiles to absolute levels using either an absorption measurement or the results from a detailed kinetics flame calculation. Further corrections, making use of flame calculation results, will be applied, if needed, to account for variations in the local quenching rates in the flame.

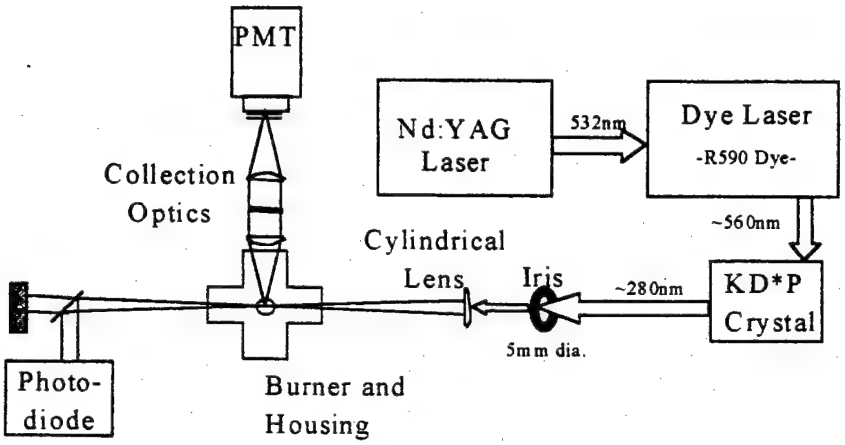

Opposed Jet Burner - LIF System Schematic

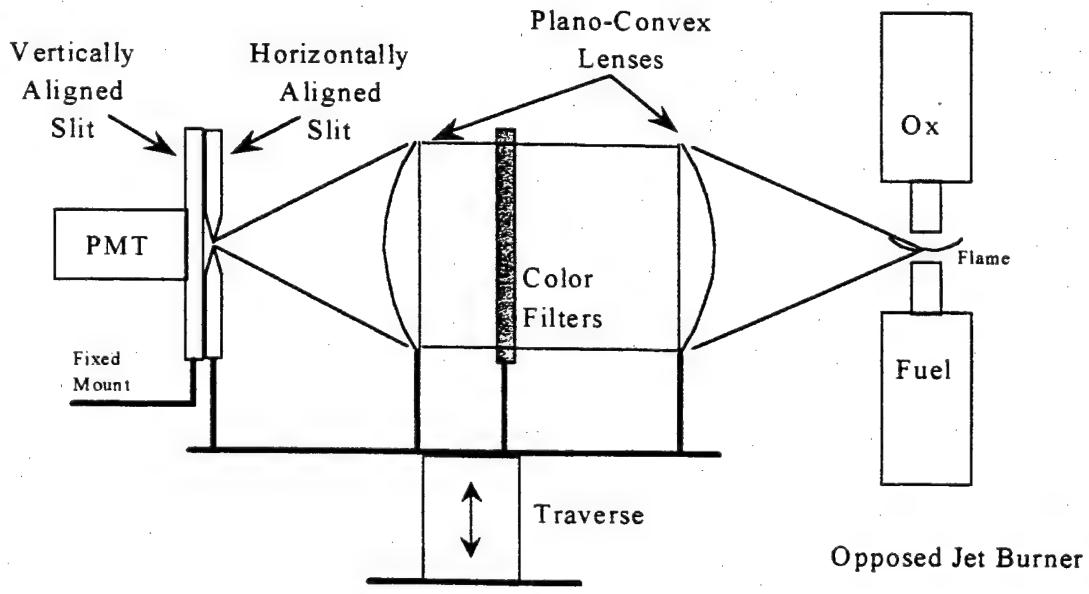

Configuration of Collection Optics

Fig. 3 Optics for Laser-Induced Fluorescence Experiments

III A 6. Droplet Size Measurements

Droplet size and velocity measurements were performed at the Combustion Dynamics Section (Code 6185) of the Naval Research Laboratory, using their Dantec Fiber Particle Dynamics Analyzer (FiberPDA), consisting of a FlowLite integrated laser-optics system, a Fiber PDA 58N70 detector unit, a Fiber PDA 58N80 signal processor, and SIZEware software v. 2.4.

All droplet size measurements, unlike vapor-phase experiments, were conducted at room temperature, and without any counterflow or sheath flow. Two configurations were used. For DMMP measurements, the configuration was as described in Section III A 4, but with the ground electrode located 5 cm from the exit of the flow tube. For measurements with aqueous solutions of PCCs, a different electrode, with ID of 0.9 cm (as opposed to 0.95 cm) was used, and the ground electrode was located at the exit of the flow tube. In all cases, the relative axial positions of the capillary and ground electrode remained the same. Droplet size measurements were taken outside the flow tube, with the probe volume roughly 5 cm below the ground electrode in all cases.

The PDA was operated in the refraction scattering mode with the laser light polarized parallel to both the plane of the fringes and the scattering flame. The measurements were taken at an angle 30° away from forward scattering. With the PDA, we obtained simultaneous measurements of the component of the droplet velocity parallel to the flow axis and the droplet diameter. Velocity measurements had an uncertainty of ±0.03 m/s. The PDA contributed an uncertainty in individual droplet measurements of ±2 μm for the DMMP droplets and ±7 μm for the droplets of water solutions of phosphorus-containing compounds. (Different aperture sizes were used for DMMP and aqueous solutions, to optimize results for the different droplet sizes produced.) There was an additional, systematic, error in droplet diameter of roughly 10% for the aqueous solutions because their indices of refraction were not known.

III B. Gas-Phase Extinction Results

We performed extinction measurements with two new phosphorus-containing compounds, diethyl methylphosphonate (DEMP, $P(=O)(-CH_3)(-OC_2H_5)_2$, CAS 683-08-9) and dimethyl phosphonate (DMP, $P(=O)(-H)(-OCH_3)_2$, CAS 868-85-9) in methane/air flames with reactants at 100 °C. In all cases, the compounds were added to the air side, in the vapor phase. The impact of these compounds on the global extinction strain rate was very similar, on a molar basis, to that of the phosphorus-containing compounds that we have tested previously, DMMP and trimethyl phosphate (TMP, $P(=O)(-OCH_3)_3$, CAS 512-56-1). Extinction results for all four compounds are shown in Fig. 4, with literature values for CF_3Br shown for comparison.

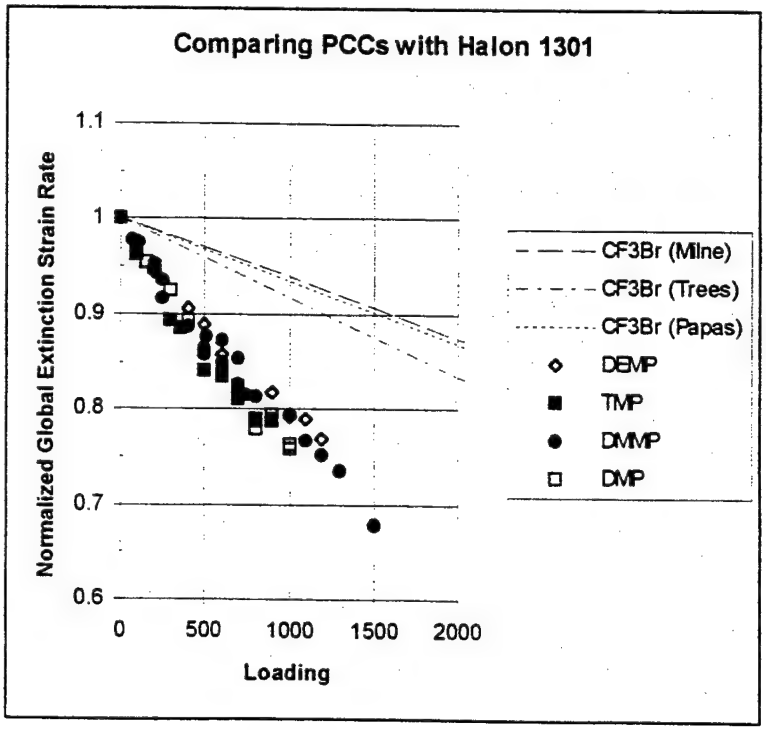

Fig. 4. Normalized global extinction strain rates for four phosphorus-containing compounds, with literature values for CF_3Br, for comparison.

The very similar molar flame suppression effectiveness observed for all four PCCs tested to date supports the idea that suppression involves phosphorus-containing species created in or near the flame. This hypothesis, if correct, suggests that PCCs can

be selected as halon replacements on the basis of physical or toxicological properties, with flame suppression effectiveness largely determined by phosphorus loading.

III C. Identification of Stable Byproducts

We have identified several stable products and byproducts of DMMP (initial loading: 500 ppm in air stream) in a non-premixed methane/air opposed-jet flame. The following compounds were detected:

Table 1. Stable compounds detected as combustion products of DMMP

methyl methylphosphonate	$P(=O)(-CH_3)(-OCH_3)(-OH)$
dimethyl phosphate	$P(=O)(-OCH_3)_2(-OH)$
monomethyl phosphate	$P(=O)(-OCH_3)(-OH)_2$
methylphosphonic acid	$P(=O)(-CH_3)(-OH)_2$
phosphonic acid	$P(=O)(-H)(-OH)_2$
phosphorous acid	$P(-OH)_3$
orthophosphoric acid	$P(=O)(-OH)_3$

Some additional GC/MS peaks remain unidentified. Some of the identified species may represent hydration products of other species. Specifically, the last five compounds listed may represent CH_3OPO_2, CH_3PO_2, HPO_2, HOPO, and $HOPO_2$, respectively. Repeatable positioning of the probe in the flame was not achieved, so the measurements did not give repeatable information about the quantities of these species. No systematic differences were observed between flames with higher and lower strain rate, or between air-side doping and previous work where the DMMP was introduced on the fuel side of the flame. The same species were also observed in previous work with a premixed flat-flame burner doped with DMMP (Rapp et al., 1997).

III D. Health Effects Assessment (J.W. Gillett)

We focus on assessing the neurotoxicity of the combustion products and byproducts of phosphorus-containing flame suppressants. These combustion products include strong acids, e.g. orthophosphoric acid, that are highly toxic via inhalation.

However, this type of toxicity is not unique to PCCs: CF_3Br produces similarly hazardous acid compounds (HF, HBr) upon combustion. It appears that, for a highly effective flame suppressant, the quantity of acid compounds typically produced is low enough to be acceptable. Thus the present assessment focuses on risks that are specific to phosphorus-containing compounds.

Toxicologically it is critical to know if there were any acid anhydrides (e.g., pyrophosphate and analogs) among the uncharacterized residue of unidentified compounds. Another concern related to the practical use of PCC flame suppressants is the possibility of producing halophosphonates. Neurotoxic intermediates can be generated in a cooling plume of combustion products. If F is present, methyl group transfer to nucleic acids (the putative first step in carcinogenicity and mutagenicity of such compounds) is enhanced for trimethyl phosphate (Ogilvie et al., 1979). These considerations would recommend against the use of fluorinated phosphorus compounds, or the joint use of PCCs with HFCs for fire fighting.

Absent acid anhydrides and halophosphonates, the toxic threat of the identified residue is extremely modest. All of the identified compounds have moderately low acute oral toxicity to rats of >5000 mg/kg (24-h observation) and no toxic threshold or upper limit found (or even recorded as sought). Esters of methylphosphonate and dimethyl phosphate can be used, respectively, as human or pesticidal neurotoxins. Dimethyl phosphate (DMP) and methylphosphonic acid (MPA) serve, respectively, as stable urinary markers of exposure to agents such as the common insecticides methyl parathion, azodrin, and dichlorvos (Morgan et al. 1977; Reid and Watts, 1981) and the chemical warfare agents sarin, soman and VX (Katagi et al., 1997; Minami et al. 1998). Analysis of urine for these compounds has been incorporated into a variety of surveillance procedures, with possible adverse consequences if these compounds are produced from non-neurotoxic flame suppressants. If a worker were have these metabolites in his/her urine, then a physician might presume prior exposure to the insecticides (even in the absence of other symptomology) and might prescribe treatment with atropine (which itself has risks) or therapy with an antidote such as 2-PAM (Gough and Shellernberger, 1977). It would be important for the examining physician to know whether the worker

actually was using or applying any of the known PCC flame suppressants from which these simple pieces can be generated, in order to avoid prescribing these treatments.

Alkyl phosphonates are not naturally occurring, but are widely distributed among industrial agents in addition to being used in insecticides. In any study of a work environment where there is an opportunity of sustained and intense exposure to the identified compounds, the research should be preceded by a series of baseline tests for serum cholinesterase level, hepatic function, and visual acuity, all known to be disturbed by various organophosphonates and organophosphate compounds. Because some DMP metabolic derivatives (Johnson, 1978) are capable of neurotoxic esterase inhibition (a phenomenon associated with the ataxia caused by triarylphosphates), but do not cause the ataxia themselves, there are still unanswered questions about the safety of any situation in which such compounds might be formed.

III E. Emission Spectroscopy

III E 1. Spectra

Figure 5 shows sample spectra taken in with the high-blaze grating, for a methane-air flame (a=300 1/s) with and without 300ppm of DMMP. The flame image was centered on the entrance slit. The predominant feature of the doped spectra is a strong broadband emission that ranges from approximately 350nm to >600nm. This emission has been attributed to PO_2 and to an oxygen- and hydrogen-containing phosphorus radical, possibly HOPO (Hamilton and Murrells, 1986). In addition to the C_2 and CH features visible in the undoped flame the doped flame, weak features near 325nm and 345nm can be seen in the doped spectrum. The 325nm peak is attributed to PO. The peak at 345nm is due to either PO or PH, both of which have band heads in that region (Pearse and Gaydon, 1976). These two phosphorus features and the broadband chemiluminescence were seen in all DMMP doped flames. Variations in intensity were observed with change in loading (0-600ppm), and change in sampling location (oxidizer or fuel side of the flame). Unfortunately, we were unable to quantify these variations using the original opposed jet burner due to lack of repeatability in optical positioning. Further studies were conducted on the 325nm PO feature using the new burner facility with a significantly improved optical arrangement. (See Section III E 2.)

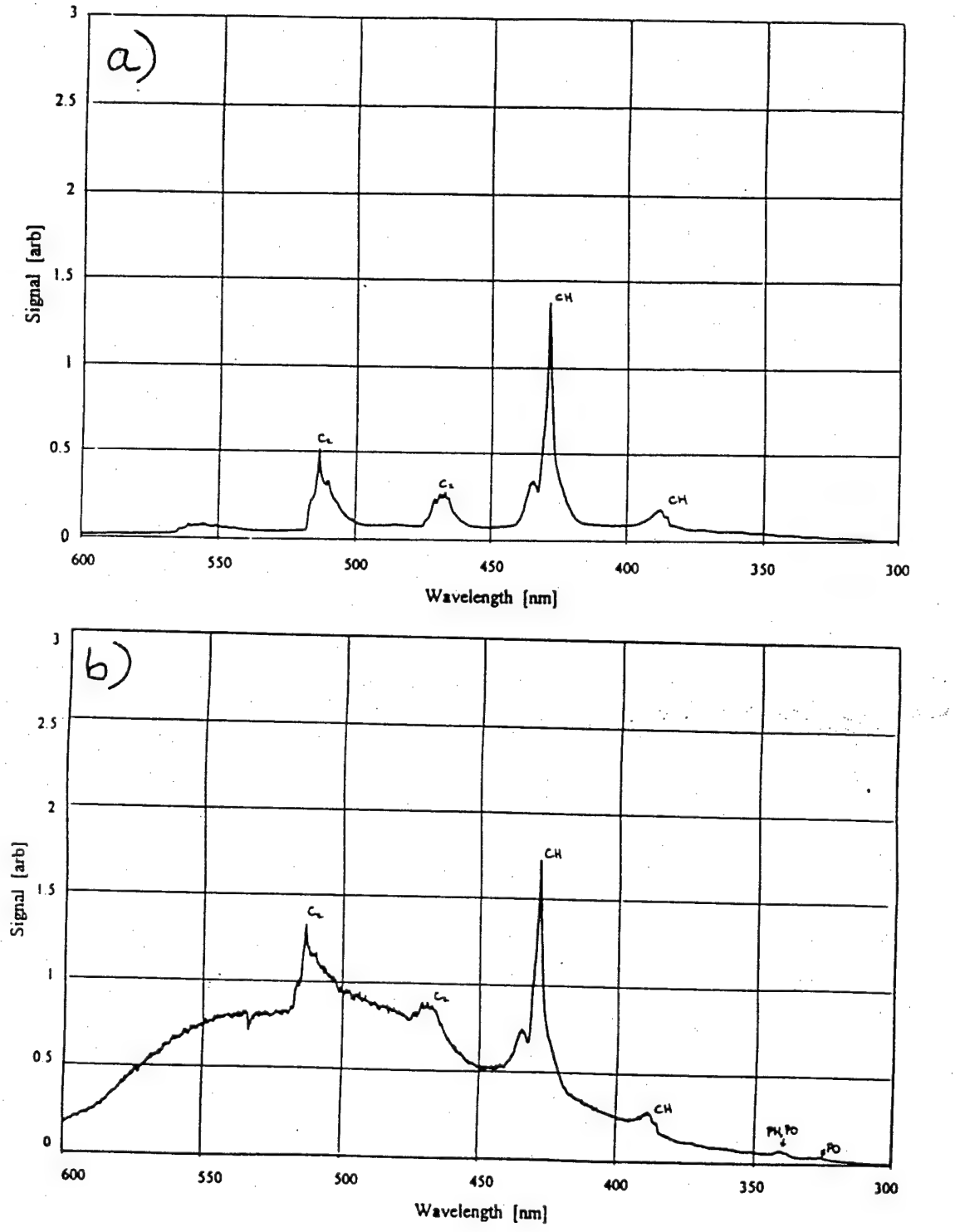

Fig. 5. Emission spectrum from opposed-jet diffusion flame a) CH_4/air; b) CH_4/air with DMMP added to air side.

III E 2. PO Profiles

Further emission spectroscopy was done to investigate the variation in emission intensity of the PO feature at 325 nm with loading, strain rate and sampling position. We studied methane-air flames with strain rates of 250 and 300 1/s (near extinction for high doping case). For each flame we acquired profiles for DMMP loadings of 0, 150, and 300ppm. Figure 6 shows the results for the 300 1/s strain rate flame, which show an increase in PO emission with loading. The 150 ppm data represent 3 separate runs indicating good repeatability. Similar trends are seen in the same figure for the 250 1/s case. These data are not corrected for photocathode response (10-15% spatial variation). The curvature of the flame provides additional difficulties in interpretation, as photons from a larger radial region of the flame are collected when the flame becomes flatter at higher strain rate. Results indicate that the strength of the PO emission feature increases monotonically with DMMP loading, and is not highly sensitive to strain rate. However, the rather high background emission observed in the absence of DMMP makes this approach less useful than anticipated as an indicator of the amount of phosphorus reaching the flame.

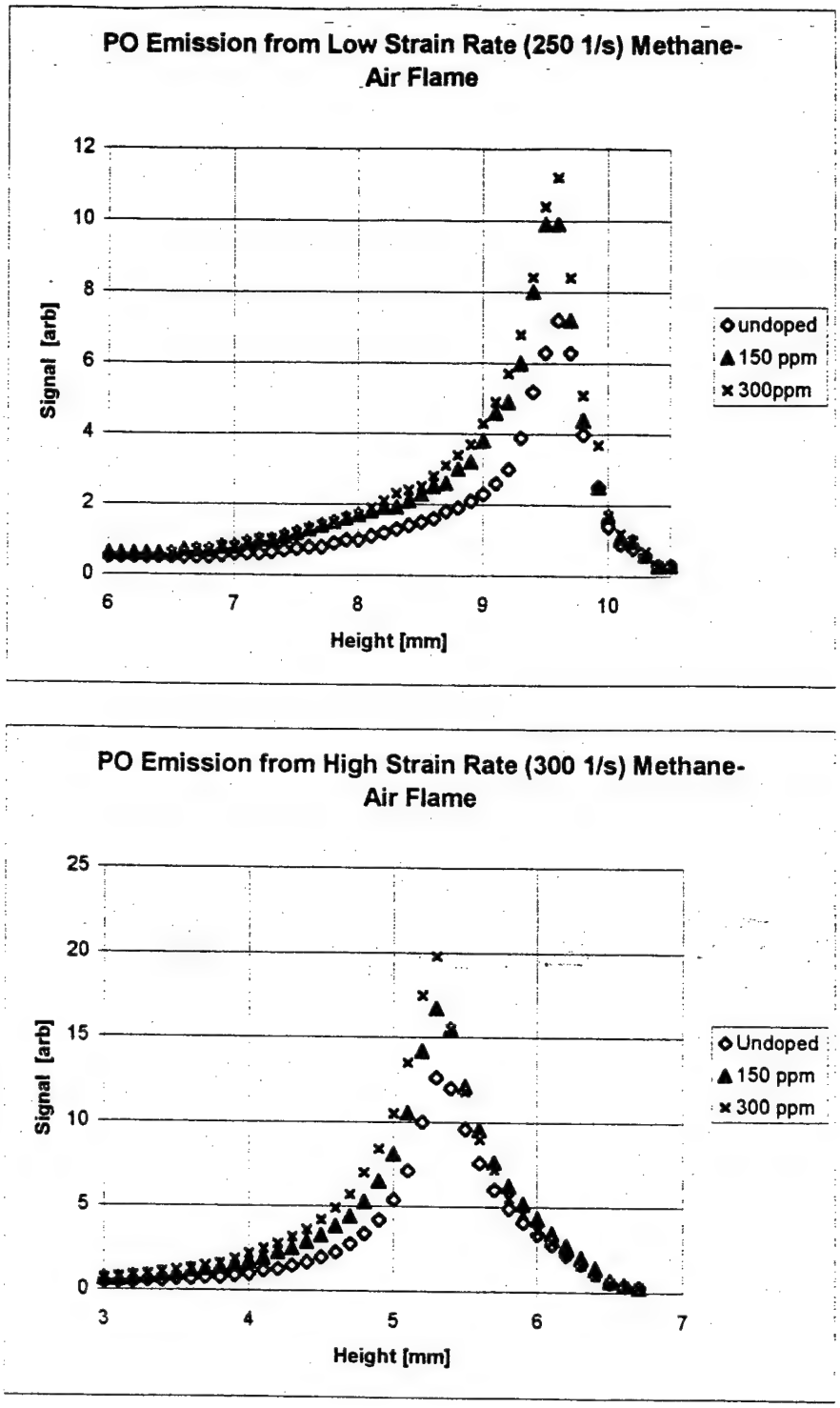

Fig. 6. Emitted light in PO spectral region.

III F. Laser-Induced Fluorescence

A profile of relative OH radical levels has been obtained in a methane/air flame with a strain rate of 300 1/s, and is shown in Fig. 7. These results are normalized by the laser intensity, but uncorrected for photocathode response or for quenching. The shape and width of the OH region are generally consistent with those observed by Skaggs et al. (1999) at lower strain rate.

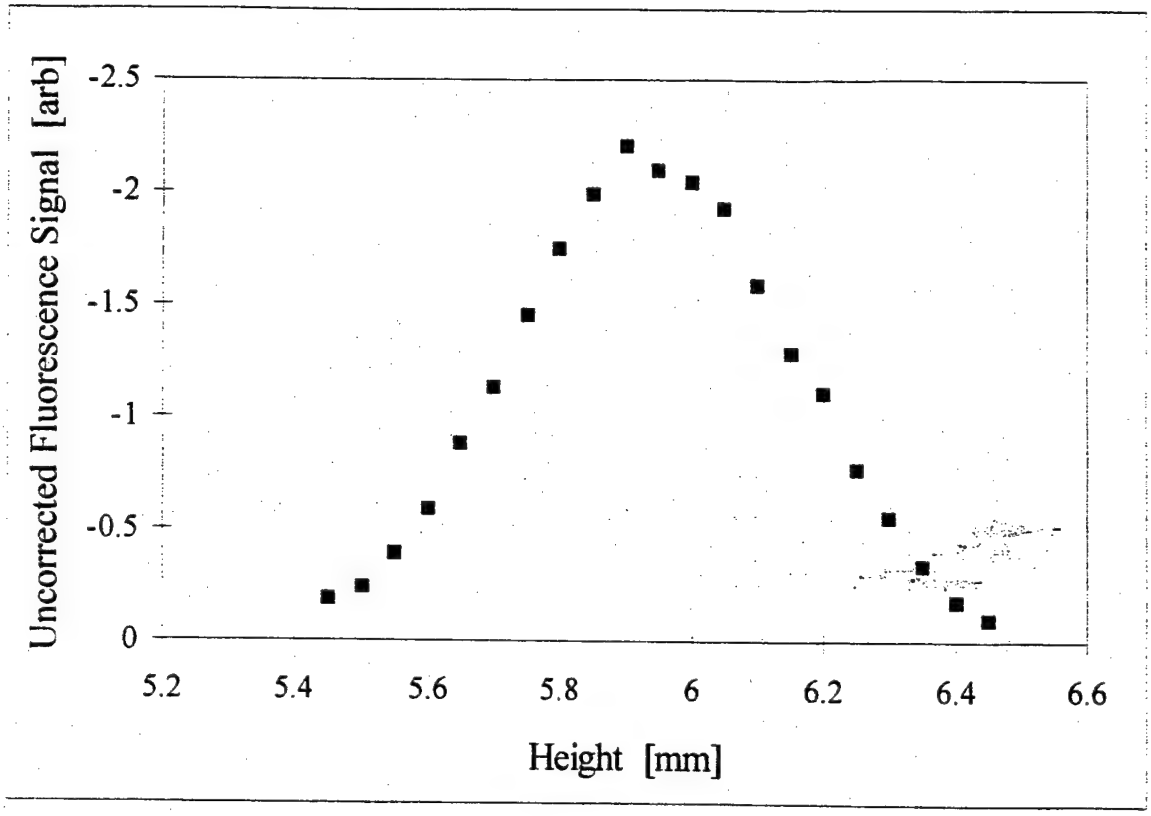

Fig. 7. Relative OH profile in methane/air flame with strain rate of 300 s-1, measured by laser-induced fluorescence

In a separate experiment, OH levels were measured without spatial resolution, with the entire flame image focused on the detector. In these, preliminary, measurements conducted on the same methane/air, 300 1/s strain rate flame, OH levels were seen to decrease with the addition of just 75 ppm DMMP to the air side.

III F. Laser-Induced Fluorescence

A profile of relative OH radical levels has been obtained in a methane/air flame with a strain rate of 300 1/s, and is shown in Fig. 7. These results are normalized by the laser intensity, but uncorrected for photocathode response or for quenching. The shape and width of the OH region are generally consistent with those observed by Skaggs et al. (1999) at lower strain rate.

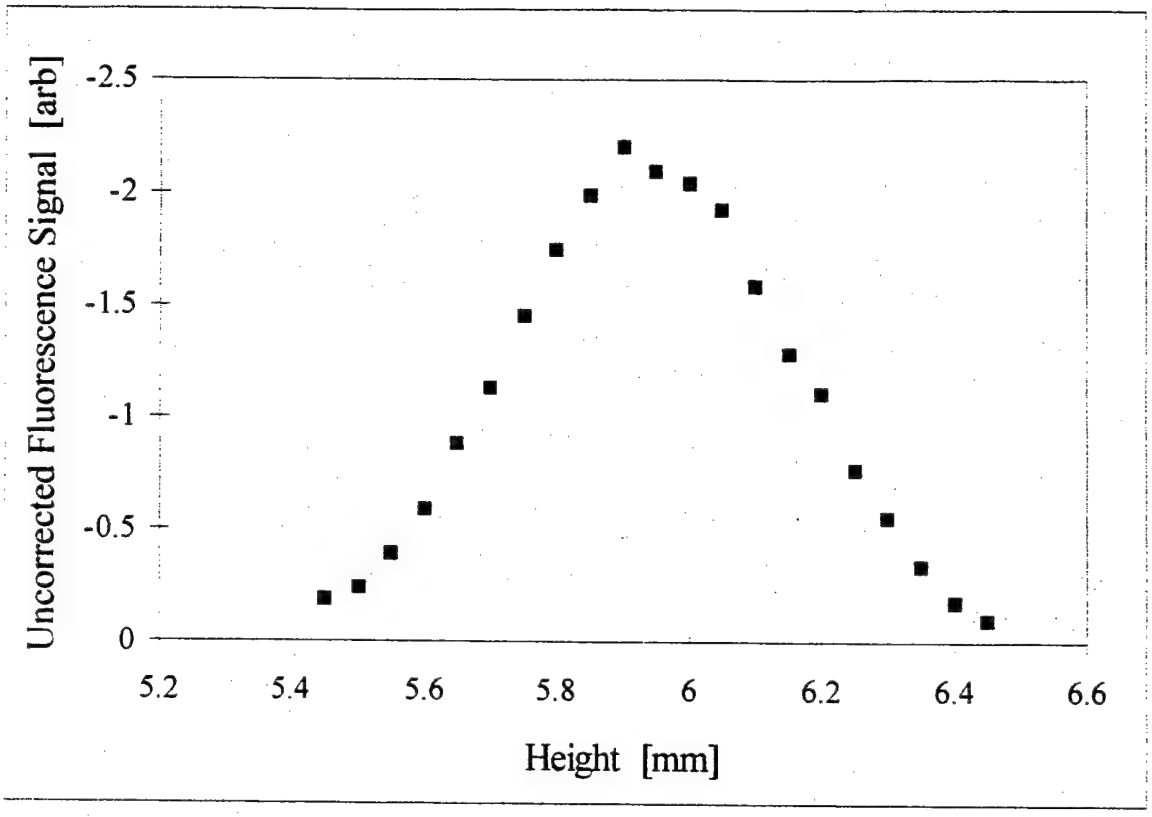

Fig. 7. Relative OH profile in methane/air flame with strain rate of 300 s-1, measured by laser-induced fluorescence

In a separate experiment, OH levels were measured without spatial resolution, with the entire flame image focused on the detector. In these, preliminary, measurements conducted on the same methane/air, 300 1/s strain rate flame, OH levels were seen to decrease with the addition of just 75 ppm DMMP to the air side.

III G. Choice of Electrospray Conditions

We had originally intended to characterize the electrospray apparatus with inert liquids such as water. However, the importance of liquid properties in determining electrospray performance (Fernández de la Mora and Loscertales1994; Gañan-Calvo et al., 1997) made it clear that it would be more useful to perform tests with the PCCs that would be ultimately used for extinction measurements. Liquids sprayed were DMMP [CAS 756-79-6], phosphonic acid [CAS 10294-46-1] in solution (42% by mass in water) and methylphosphonic acid [CAS 993-13-5] in solution (28% by mass in water).

A laser sheet was used to visualize the spray under different operating conditions. An electrospray can operate in different "modes" depending on liquid properties, liquid flowrate, and applied voltage (Cloupeau and Prunet-Foch, 1994). Visualization was used to observe the spray to determine which mode occurs. The goal is to identify conditions producing the stable cone-jet mode of operation, the mode which is the most stable and which can generate the most nearly monodisperse droplet distribution. For each liquid, its flow rate was varied from 5 to 30 μl/min. For each liquid flow rate, the voltage was varied over a 1000-V range, in 100V increments, to observe the different spray modes. The voltages chosen were such that the most stable spray was produced near the middle of the voltage range. The appearance of a small cone on the tip of the capillary, accompanied by a stable spray, was taken to indicate operation in the stable cone-jet mode. At lower voltages, dripping from the capillary tip occurred, and at higher voltages, the spray would sputter although a cone might be visible. It was often difficult to determine when the dripping ended or sputtering began since the frequency of these events would only gradually change with voltage. In addition, no magnification was used, so it was difficult to observe small perturbations. All tests were done at two temperatures: room temperature and 95 °C. The main observable change with temperature was that there was less condensation on the walls of the tube at the elevated temperature. Also, the voltage region in which the stable cone-jet mode was observed shifted slightly, the direction and amount of shift being compound dependent.

III H. Electrospray Droplet Sizing and Extinction Measurements

The laser sheet visualization experiments provide information on the stability of the spray and the presence of a Taylor cone, but not on the droplet size distribution. Droplet size can be estimated from various proposed scaling laws (Fernández de la Mora and Loscertales1994; Gañan-Calvo et al., 1997)), or can be measured.

The use of scaling laws requires knowledge of the physical properties of the liquid to be sprayed. Several relevant properties are not available in the literature for the PCCs and aqueous solutions of interest. We have measured some of the relevant physical properties for DMMP: 1) viscosity, 2) surface tension and 3) conductivity. The measurement of viscosity was done using a Gilmont Falling Ball Viscometer (bought from Cole-Parmer) and found to be 1.84 ± 0.01 cP (centiPoise). The surface tension was measured using the capillary rise method, giving 0.026 N/m. In the literature (Arbuzov and Vinogradova, 1947), 0.0367 N/m is reported. This demonstrates the uncertainty in estimation of the contact angle is quite large. Finally, the conductivity was found to be 2.6E-3 $(\text{ohms m})^{-1}$ using a Freas-type conductivity cell, coupled with a conductivity bridge, with 0.01 M KCl as a standard. The uncertainty here is estimated to be about 10% (± 0.3E-3). We were not able to measure the dielectric constant for DMMP, but the predicted dependence of droplet size on this parameter is weak.

Table 2 shows the DMMP droplet sizes predicted by the correlation of Gañan-Calvo (1997), using our measured property values. The range of flowrates is the range that appeared to produce a stable cone jet, and was used in particle sizing measurements. For each flowrate, two predicted sizes are listed, representing extreme possible values of the dielectric constant. These values differ by roughly a factor of two.

Table 2. Predicted DMMP droplet size, using correlation of Gañan-Calvo (1997).

dielectric constant	flowrate DMMP	predicted droplet size
(-)	(μl/min)	(μm)
2	5	1.1
2	25	1.8
80	5	2.2
80	25	3.7

PDA measurements were roughly consistent with these predictions, indicating that electrospray of DMMP produced droplets with mean diameters ranging from 1.5 to 5.6 μm depending on the applied voltage and the DMMP flowrate. Although conditions included those producing the most stable spray possible, with a Taylor cone visible, the droplet distribution was not monodisperse. Standard deviations of droplet size distribution were as high as 10 μm, though generally considerably smaller. A typical PDA droplet size and velocity distribution for DMMP is shown in Fig. 8.

Our knowledge of properties of the aqueous solutions of methylphosphonic acid and phosphorous acid is insufficient to predict electrospray droplet sizes. Droplet sizes distributions were measured with PDA, and were very different from the DMMP results. Mean diameters varied between 97 and 275 μm. Size distributions varied widely: Under some conditions, the spray was quasi-monodisperse, with standard deviation below 3% of the mean droplet diameter. In other cases, the distribution was very broad (standard deviation > 50 μm) or clearly bimodal. An example of a monodisperse case is shown in Fig. 9.

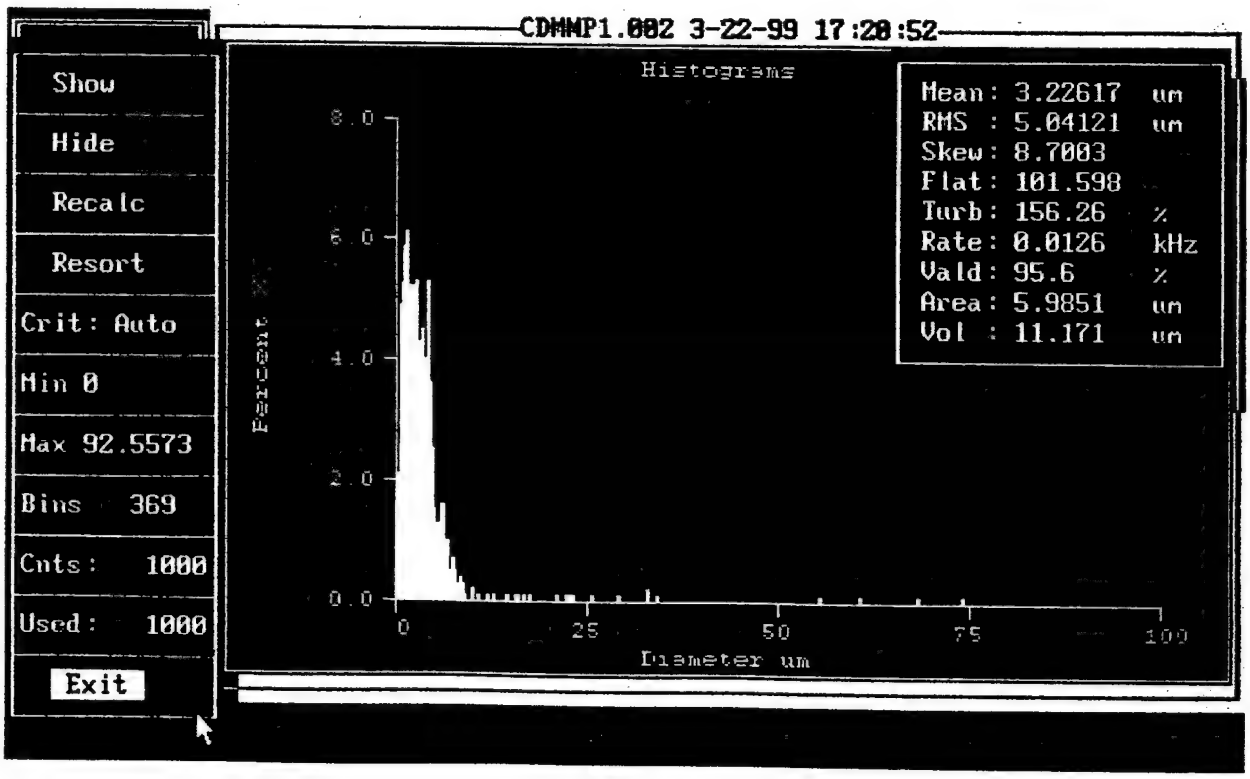

Fig. 8. Droplet diameter measurements for DMMP. liquid flowrate: 15 µl/min; applied voltage: 3000 V; air flowrate: 2 slpm.

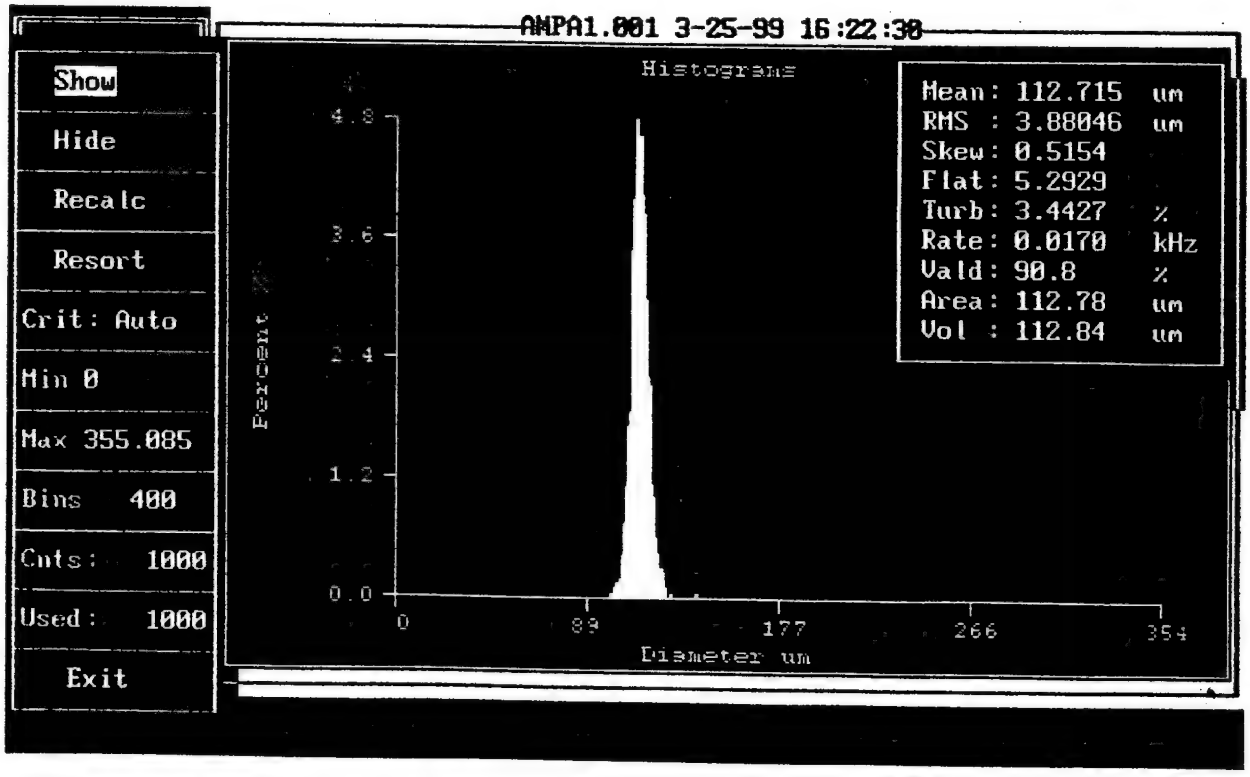

Fig. 9. Droplet diameter measurements for aqueous solution of methylphosphonic acid. liquid flowrate: 25 µl/min; applied voltage: 4000 V; air flowrate: 1 slpm.

We used the electrospray apparatus to perform preliminary extinction measurements with DMMP delivered to the opposed-jet diffusion flame as droplets. DMMP was delivered at several flowrates corresponding to loadings between 300 and 4000 ppm. These results are shown in Fig. 10. As the highest loading achieved reliably with vapor-phase delivery was 1500 ppm, this represents an advance in the operating conditions achievable with the burner. The normalized global extinction strain rate was lower for droplet delivery than for vapor-phase delivery, at the loadings for which a comparison was possible. The droplet data exhibited nonlinear behavior, with effectiveness per mole DMMP decreasing as DMMP loading increased above about 1000 ppm. At 4000 ppm, the normalized global extinction strain rate was 0.45. It is important to realize that droplet size is expected to increase as liquid flowrate increases at fixed applied voltage. Thus the droplet delivery data represent different atomization conditions as well as different loadings. Furthermore, electrospray conditions for these tests were somewhat different from those used in the droplet sizing and flow visualization measurements reported above, making it impossible to attribute these extinction results to a particular droplet size distribution.

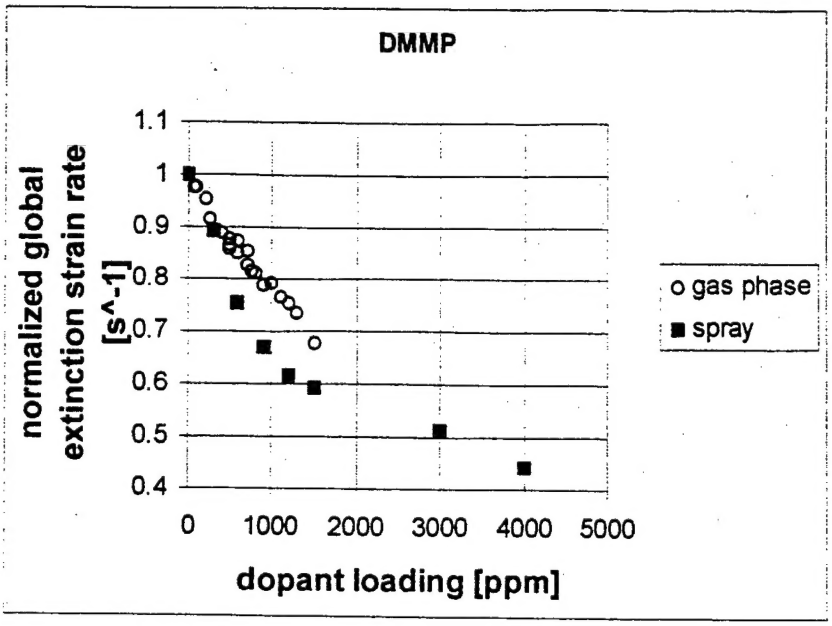

Fig. 10. Extinction results for DMMP added to the air side of a methane/air flame. Open symbols represent vapor-phase delivery (previous results); Closed symbols represent droplet delivery.

IV. UNRESOLVED TECHNICAL PROBLEMS

Several problems will need to be resolved before electrospray can be used as planned, to deliver PCCs and their aqueous solutions in the form of monodisperse sprays of small droplets. Currently, electrospray of aqueous solutions of PCCs produces very large droplets, leading to large uncertainties in the PCC loading effectively reaching the flame and affecting its chemistry. Electrospray of DMMP produces small droplets but non-monodisperse sprays. Possible approaches to overcoming these problems are discussed in Section V. below.

V. RECOMMENDATIONS FOR ADDITIONAL RESEARCH

A more powerful technique for visualizing the electrospray is needed, to ensure that cone-mode electrospray is in fact achieved under the conditions of our work. Stereo microscope systems have been widely used for spray and cone visualization, and can

provide more reliable information about the mode of operation. Property measurements for the aqueous solutions of PCCs are needed, in order to determine whether the large droplets observed here are consistent with literature predictions. If so, manipulating properties such as electrical conductivity and surface tension with additives may lead to the production of small droplets, as desired.

Once the electrospray difficulties have been resolved, it would be worthwhile to perform extinction measurements with several new PCCs that have been impossible to deliver to the flame as vapors. These measurements will provide a stronger test of the hypothesis that the chemical form of the parent phosphorus-containing molecule has little effect on the flame-suppression effectiveness. If this hypothesis is correct, it opens the way to the design of phosphorus-containing molecules for optimal toxicological properties and materials compatibility, with the assurance that flame-suppression effectiveness is likely to be high. Electrospray may prove useful for the delivery of a broader range of low-volatility potential halon replacements as well, and may be of particular use in testing chemicals used to enhance the effectiveness of water mists.

Measurements of levels of OH and of phosphorus-containing radicals in the flame zone of doped flames are also of interest. Quantitative measurements of the transient species responsible for the flame chemistry and its disruption will provide useful tests of proposed mechanisms of flame suppression by phosphorus. This information has the potential of improving the selection or design of flame suppressants.

VI. CONCLUSIONS

Our findings support the hypothesis that PCCs' flame suppression is insensitive to their initial chemical form, and is probably due to effects on radical chemistry in the flame zone. However, the experiments reported here do not provide a definitive test of that hypothesis.

No highly neurotoxic toxic combustion byproducts of DMMP were identified. Such a finding would have disqualified DMMP, and probably most similar compounds, from consideration as halon replacements. Corrosive acid combustion products were identified, and are likely to pose a threat comparable to that resulting from halon flame suppression.

Preliminary results of OH LIF and electrospray droplet delivery indicate that these techniques can contribute to future studies of PCC flame suppression.

VII. ACKNOWLEDGMENTS

The authors acknowledge several very useful interactions with Drs. J. Fleming, B. Williams, and E. Zegers in the Combustion Dynamics Group of the Naval Research Laboratory. The assistance of Mr. Kevin Ring and Brendan Lippman is also appreciated.

VIII. REFERENCES

Arbuzov, B.A., and Vinogradova, V.S., *Bull. Acad. Sci. U.R.S.S., Classe. Sci. Chim.* (in Russian) pp. 459-472 (1947).

Cloupeau, M., and Prunet-Foch, B., *J. Aerosol Sci.* v. 25, pp. 1021-1036 (1994).

Fernández de la Mora, J., and Loscertales, I.G., *J. Fluid Mech.* v. 260, pp. 155-184 (1994).

Fisher, E.M., Gouldin, F.C., Jayaweera, M.A., and MacDonald, M.A., Flame Inhibition by Phosphorus-Containing Compounds, Final Technical Report to SERDP, DARPA contract MDA972-97-M-0013, March 1998.

Gañan-Calvo, A.M., Davila, J., and Barrero, A., *J. Aerosol Sci.*, v. 28, pp. 249-275 (1997).

Gough, B.J., and Shellernberger, T.E., *Drug Chem.Toxicol.* v. 1, pp. 25-43 (1977).

Grudno, A., and Seshadri, K., *Combust. Sci. Technol.* v. 124, pp. 311-330 (1997).

Hamilton, P.A., and Murrells, T.P., *J. Phys. Chem.* v.90, pp. 182-185 (1986).

Johnson, M.K. (1978). *Arch. Toxicol.* v. 41, pp. 107-110 (1978).

Katagi, M, Nishikawa, M., Tatsuno, M. and Tsuchihashi, H. *J. Chromatogr. B. Biomed. Sci. Appl.* v. 98, pp. 81-88 (1997).

Milne, T.A., Green, C.L., and Benson, D. K., *Combust. Sci. Technol.*, v. 56, pp. 1-22 (1987).

Minami, M., Hui, D.M., Wang, Z., Katsumata, M., Inagaki, H., Li, Q., Inuzuka, S., Mashiko, K., Yamamoto, Y., Ootsuka, T., Boulet, C.A., and Clement, J. G., *J. Toxicol. Sci.* v. 23 (Suppl. 2), pp. 250-254 (1998).

Morgan, D.P., Watts, H.L., Slach, E.F., and Lin, L.I, *Arch. Environ. Contam. Toxicol.* v. 6, pp. 159-173 (1977).

Ogilvie, K.K., Beaucage, S.L., Gillen, M.F., and Endwistle, D.W., (1979). *Nucleic Acids Res.* v. 6, pp. 2261-2273 (1979).

Papas, P., Fleming, J.W., and Sheinson, R.S., *26th Symposium (International) on Combustion*/ The Combustion Institute, pp. 1405-1412 (1996).

Pearse, R. W. B., Gaydon, A. G., *The Identification of Molecular Spectra*, 4th edition, John Wiley and Sons, NY, 1976.

Rapp, D.C., Nogueira, M.F.M., Fisher, E.M., and Gouldin, F.C., *Environm. Engin. Sci.*, v. 14, pp. 133-140 (1997).

Reid, S.J. and Watts, R.R., *J. Anal. Toxicol.* v. 5, pp. 126-132 (1981).

Skaggs, R.R., Daniel, R.G., Miziolek, A.W., and McNesby, K.L., "Spectroscopic Studies of Inhibited Opposed Flow Propane/Air Flames," presented at the First Joint Meeting of the U.S. Sections of the Combustion Institute, Washington, DC, March 14-17, 1999.